Localized-to-itinerant electron transition in $Sr_2Ir_{1-x}Ru_xO_4$

R. J. Cava and B. Batlogg
AT&T Bell Laboratories, 600 Mountain Avenue, Murray Hill, New Jersey 07974

K. Kiyono and H. Takagi
Department of Applied Physics, University of Tokyo, Tokyo 113, Japan

J. J. Krajewski, W. F. Peck, Jr., L. W. Rupp, Jr., and C. H. Chen
AT&T Bell Laboratories, 600 Mountain Avenue, Murray Hill, New Jersey 07974
(Received 14 October 1993; revised manuscript received 27 January 1994)

Sr_2IrO_4 and Sr_2RuO_4 are both K_2NiF_4-structure oxides. Sr_2IrO_4 is a weakly ferromagnetic insulator and Sr_2RuO_4 a paramagnetic metal. The $Sr_2Ir_{1-x}Ru_xO_4$ solid solution displays surprising physical properties. On the substitution of Ru to Sr_2IrO_4, the Ru first exhibits its expected $S=1$ local magnetic moment, but at a critical Ru concentration of $x \cong 0.7$ the local moment disappears, the apparent density of states at E_F increases, and an insulator-to-metal transition occurs. These changes in physical properties are accompanied by a change in the crystallographic cell parameters.

INTRODUCTION

While much attention has recently been focused on the 3*d* transition-metal oxides, detailed properties of the 4*d* and 5*d* metal oxides remain largely unexplored. Transition-metal oxides with the layered K_2NiF_4 structure type are of particular interest due to the variety of unusual structural and magnetic properties they display.[1] Though commonly known for the first-row transition metals, a handful of 4*d*- and 5*d*-based K_2NiF_4-type oxides are also known.[2] Of these, Sr_2RuO_4 and Sr_2IrO_4 are exceptional materials; the former due to its good metallic conductivity, and the latter, on the contrary, due to its insulating nature, unexpected for octahedrally coordinated Ir^{4+} (five 5*d* electrons) which is expected to yield a partially filled t_{2g} band. In this study, we have prepared and characterized the $Sr_2Ir_{1-x}Ru_xO_4$ solid solution, with the intention, in part, of looking for superconductivity at the composition of the metal-insulator (*M-I*) transition. As for many of the oxide systems we have studied, the *M-I* transition occurs without the appearance of superconductivity. We have observed, however, that as Ru is substituted for Ir in Sr_2IrO_4 it exhibits its full local $S=1$ moment up to a critical concentration beyond which the local moment then begins to disappear. The behavior of this system is considerably different from what is generally observed for Ru^{4+} in oxides, typified by $Sr_{1-x}Ca_xRuO_3$,[3,4] where full Ru local moments are virtually exclusively found. The disappearance of the local moment in $Sr_2Ir_{1-x}Ru_xO_4$ is associated with an increase in the apparent density of states (by an increase in the temperature-independent susceptibility χ_0), and, probably, the insulator-to-metal transition. At the same time, the crystallographic *c* axis, a measure of the structure perpendicular to the planes, collapses, and the *a* axis, a measure of in-plane structure, saturates at a minimum value. The results also show that for Sr_2RuO_4 itself local-moment behavior might have been expected, but instead an itinerant-spin state occurs.

EXPERIMENTAL

Although $Sr_2Ir_{1-x}Ru_xO_4$ are refractory materials, they must be synthesized at relatively low temperatures to avoid the volatilization of IrO_2. Starting materials $SrCO_3$, IrO_2, and RuO_2 were mixed in proportions to span the solid-solution series and heated in flowing O_2. Typical heating schedules were 900 °C, 24 h; 1000 °C, 60 h; and 1100 °C, 60 h, with many intermediate grindings. Long times and repeated grindings were necessary to insure homogeneity: heating at higher temperatures, up to 1150 °C, was possible for high Ru contents without decomposition. Because of the low temperatures necessary for the synthesis of single-phase materials, polycrystalline pellets were not dense (70–80 % theoretical density).

Magnetic properties were measured on powders and on polycrystalline pellets between 4.2 and 400 K in a superconducting quantum interference device (SQUID) magnetometer in a field of 10 kOe. Resistivity measurements were made at 100 Hz in bar geometry with the four-terminal method, employing Ag paint electrodes, between 4.2 and 300 K. Due to the low density of the samples we consider the resistivity data as showing overall relative but not absolute behavior. Powder x-ray-diffraction measurements were performed on a Rigaku powder diffractometer with Cu $K\alpha$ radiation. Electron-diffraction measurements were performed on crushed powders in a JEOL 2000SS microscope.

RESULTS

With a difference in unit-cell volume of only 2% between Sr_2IrO_4 and Sr_2RuO_4, the solid solution $Sr_2Ir_{1-x}Ru_xO_4$ might be expected to show ideal Vegard's

 ©1994 The American Physical Society

law behavior. That is not the case. The lattice parameters for the solid solution, determined by fitting to the positions of five high-angle lines in the powder x-ray-diffraciton patterns, are presented in Fig. 1. Weak superlattice reflections were observed for Sr_2IrO_4 by electron diffraction (described further in a later section), indicating that the true unit cell is larger than that of the ideal K_2NiF_4 structure. For the purposes of comparison to Sr_2RuO_4 we consider the subcell dimensions in both the general discussion and the figures. The lattice parameters for the end members are in good agreement with those previously reported,[5,6] except for the a axis of Sr_2RuO_4 which we find to be 3.878 (not 3.870) Å. The materials are single phase for all x: there are no two-phase regions. The data show the expected Vegard's law linear shrinkage of c and a on the substitution of Ru into Sr_2IrO_4, to a composition of $Sr_2Ir_{0.4}Ru_{0.6}O_4$, where there is a sudden change in the rate of decrease of the c-axis length and a stabilization of the a-axis length at 3.878 Å. This kind of distinct change in behavior within a solid solution could be due either to electronic factors, such as a change in the filling of electronic orbitals, or to structural factors, such as buckling or twisting of the plane of MO_6 octahedra, which are well known in the K_2NiF_4 structure type.

Temperature-dependent resistivities for representative compositions, measured on polycrystalline pellets, are presented in Fig. 2. The data show Sr_2IrO_4 to be semiconducting. The transition to a metallic resistivity occurs only at very high Ru doping, between $SrIr_{0.2}Ru_{0.8}O_4$ and Sr_2RuO_4. Due to the low pellet densities, the semiconductor-to-metal transition could not be located to good compositional precision, and in fact we expect that it occurs between $Sr_2Ir_{0.4}Ru_{0.6}O_4$ and $Sr_2Ir_{0.2}Ru_{0.8}O_4$. For our Sr_2RuO_4 polycrystalline pellets, our measured resistivity, 10^{-2} Ω cm, is higher by at least an order of magnitude than that expected based on single-crystal resistivity measurements[7] which found $\rho_{ab}(300\text{ K}) \cong 10^{-4}$ Ω cm and $\rho_c(300\text{ K}) \cong 3\times10^{-2}$ Ω cm. This indicates a very high grain-boundary resistivity for our pellets, making exact determination of the composition of the M-I transition ambiguous.

The temperature-dependent magnetization data are presented in Figs. 3 and 4, as susceptibility defined by $\chi = M(H = 10\text{ kOe})/H$. All data shown have been corrected for core diamagnetism (1.06×10^{-4} emu/mole for Sr_2IrO_4 and 0.97×10^{-4} emu/mole for Sr_2RuO_4). The Sr_2IrO_4 and Sr_2RuO_4 samples show transitions to weakly ferromagnetic states at 250 and 160 K, respectively. The ordered ferromagnetic moment for Sr_2IrO_4 measured at high fields in the M vs H data is very low: $0.02\mu_B$. By magnetic characterization of other Sr, Ir oxides which might be present as impurities at very low levels, we find that for Sr_2IrO_4 the ordering is intrinsic to the phase, in agreement with previous studies.[2] The low saturated moment suggests that as in La_2CuO_4 there is a small ferromagnetic component present in an antiferromagnetically ordered spin system due to canting of the

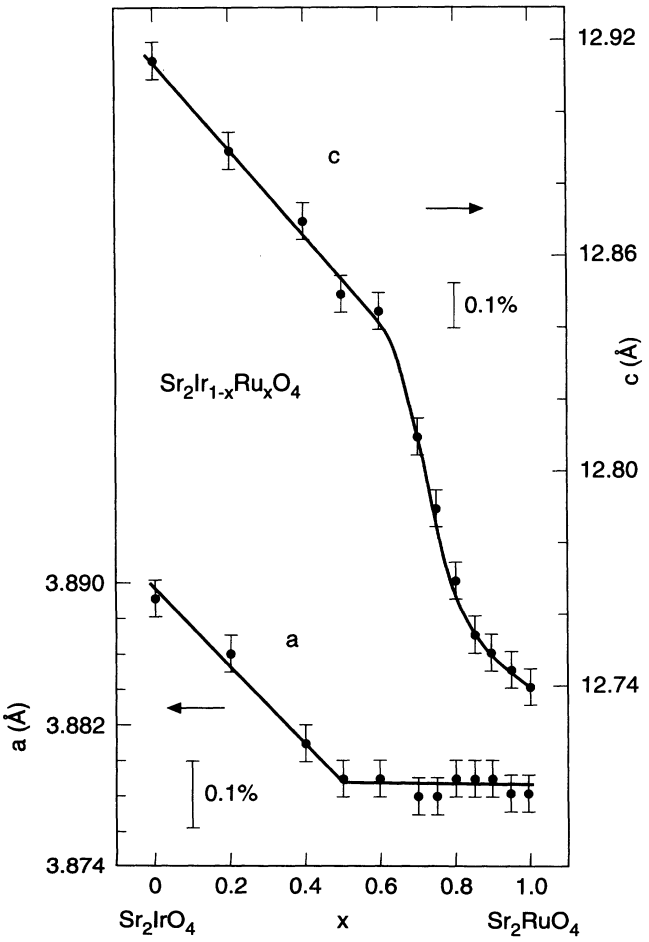

FIG. 1. Crystallographic unit-cell parameters as a function of composition in the $Sr_2Ir_{1-x}Ru_xO_4$ solid-solution series. For the sake of comparison, subcell dimensions are plotted for compositions near Sr_2IrO_4 (see text).

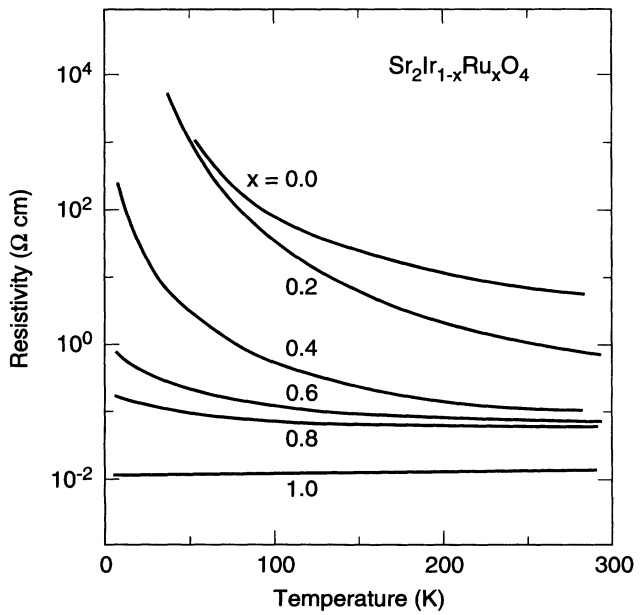

FIG. 2. Temperature-dependent resistivities for polycrystalline samples of $Sr_2Ir_{1-x}Ru_xO_4$ at composition intervals $\Delta x = 0.2$.

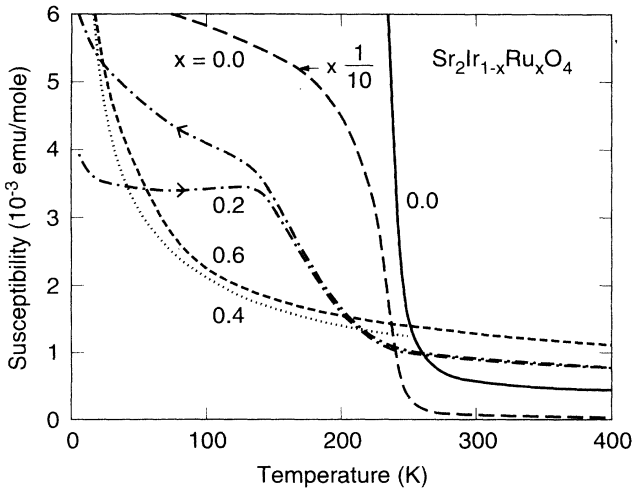

FIG. 3. Temperature-dependent magnetic susceptibilities (M/H at $H=10$ kOe) for $Sr_2Ir_{1-x}Ru_xO_4$ measured in a field of 10 kOe for $x \leq 0.6$.

ordered moments. For the Sr_2RuO_4 sample, our magnetic characterization of possible impurity phases shows that the apparent magnetic transition observed at 160 K is due to the presence of a very small amount (less than 50 ppm) of ferromagnetic $SrRuO_3$. We find no intrinsic ordering for Sr_2RuO_4, again in agreement with previous studies.[2] For some intermediate compositions, a very weak remnant of the ferromagnetic ordering of the end members is seen: the presence of small amounts of Ru in Sr_2IrO_4 appears to suppress T_c. Near Sr_2RuO_4 any change in the ferromagnetic properties is due to a change in the ppm-level impurity phase.

At temperatures above the Curie point (150–200 K), the overall $\chi(T)$ for all compositions is very similar. The high susceptibility, 10^{-3} emu/mole, is characteristic of a highly magnetic electronic system, similar to what is typically observed for 3d transition-metal oxides. To look at these data in detail, the susceptibilities above 200 K have been fit to the Curie-Weiss behavior $\chi=\chi_0+C/(T-\theta)$, where χ_0 is the temperature-independent paramagnetism, C the Curie constant, and θ the Curie-Weiss temperature. Figure 5 shows the composition dependence of the total measured susceptibility at 400 K, and the temperature-independent part of the susceptibility, χ_0. Because the value of χ_0 may be expected to depend on the temperature region of the fit, different minimum fit temperatures were employed in different fits. The variations in χ_0 and ρ_{eff} with fitting and sample preparation are shown in Figs. 5 and 6 by different symbols. The observations are seen to be independent of fitting procedure and sample preparation.

The difference between $\chi(400)$ and χ_0 shows, as a function of composition, the relative contributions of local-moment magnetism and temperature-independent paramagnetism to the total susceptibility. Local-moment magnetism is seen first to increase with increasing Ru content, and then to decrease for Ru contents greater than approximately 0.7. At the same time, the temperature-independent susceptibility is independent of Ru content up to the same critical concentration, where it then dramatically increases as the local-moment magnetism goes away. Taken as a measure of the density of states at the Fermi level, the increase in χ_0 represents an increase to a high γ (linear specific heat coefficient) for Sr_2RuO_4. The high γ must be attributed to either a highly correlated spin state for Sr_2RuO_4 or electron-electron correlation.

Figure 6 shows the correlation between the structural and magnetic properties. The upper panel shows the Curie moment per formula unit of $Sr_2Ir_{1-x}Ru_xO_4$ obtained

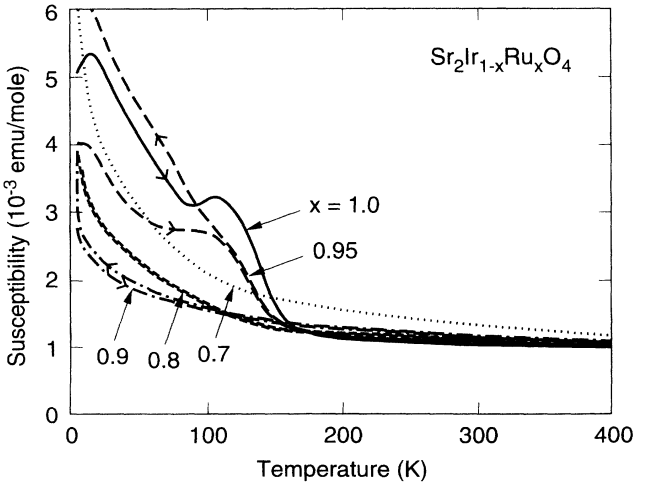

FIG. 4. Temperature-dependent magnetic susceptibilities (M/H at $H=10$ kOe) for $Sr_2Ir_{1-x}Ru_xO_4$ measured in a field of 10 kOe for $x>0.6$. The apparent ferromagnetic transition observed near Sr_2RuO_4 ($x=1.0$ and 0.95) is due to the presence of very small (50 ppm) quantities of $SrRuO_3$.

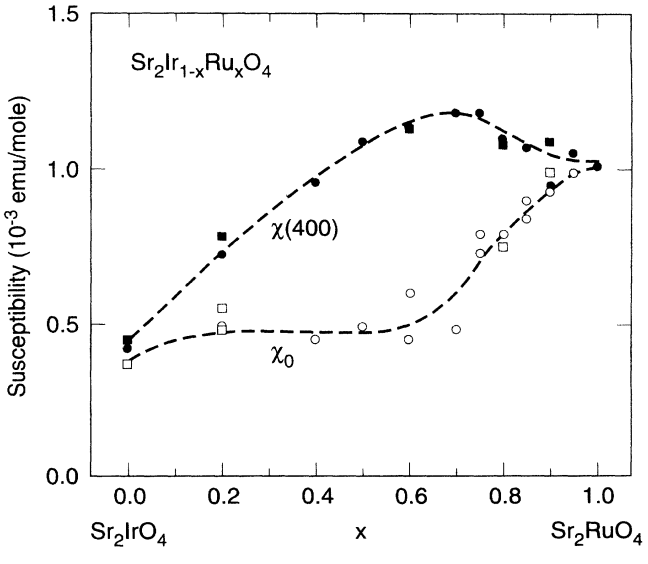

FIG. 5. Composition dependence of the total magnetic susceptibility at 400 K [$\chi(400)$] and the temperature-independent paramagnetic contribution (χ_0). At a particular composition, different symbols represent different sample preparations and identical symbols represent different fitting ranges.

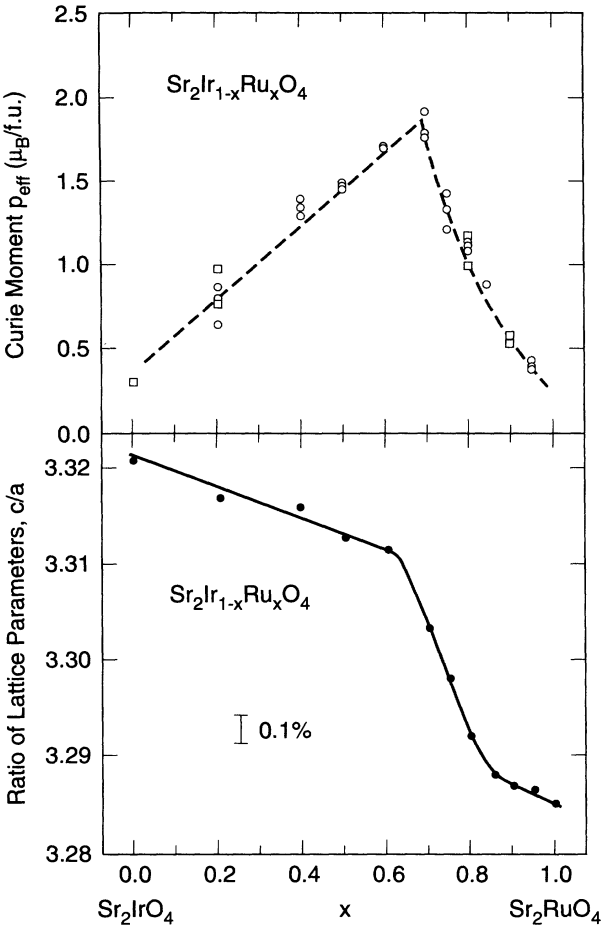

FIG. 6. Curie moment ρ_{eff} per formula unit of $Sr_2Ir_{1-x}Ru_xO_4$ (upper panel) and the crystallographic c/a ratio (lower panel) as a function of composition. For ρ_{eff} at a particular composition, different symbols represent different sample preparations and identical symbols represent different fitting ranges.

from the high-temperature $\chi(T)$ fits. The data clearly show the linear relation between observed moment and Ru concentration for $x \leq 0.7$. Extrapolation of this line to $x=1$ (pure Ru) yields the effective moment per Ru$\simeq 2.5\mu_B$/Ru, which is close to what is expected for $S=1$ Ru^{4+} in localized magnetic systems. However, as the Ru concentration increases beyond $x=0.7$ the local-moment behavior does not hold up: rather, by Sr_2RuO_4 there remains very little to the measured local Ru moment. Comparison of the upper panel of Fig. 6 and χ_0 in Fig. 5 shows that the temperature-independent paramagnetism grows dramatically with the disappearance of the local moment. The lower panel of Fig. 6 presents a plot of the crystallographic c/a ratio (determined from the data in Fig. 1) for $Sr_2Ir_{1-x}Ru_xO_4$, showing the correlation between the loss of local-moment magnetism and a decrease in the aspect ratio of the tetragonal unit cell. Detailed interpretation of the c/a ratio on an atomic scale is ambiguous without a full structural study. Electron-diffraction study of both Sr_2RuO_4 and Sr_2IrO_4 reveals that the former is indeed a simple tetragonal K_2NiF_4-structure material, but that Sr_2IrO_4 shows weak superlattice reflections suggesting a larger tetragonal cell with $a'=\sqrt{2}a_0$ and $c'=2c_0$. Such crystallographic cell increases in K_2NiF_4-structure oxides are typically due to rotations and tilts of the planes of transition-metal–oxygen octahedra. There may also be an electronic component in the behavior of c/a, reflecting a transfer of charge between various t_{2g} orbitals, but detailed structural study is needed. However, even small tilts of the metal-oxygen octahedra are known to affect physical properties profoundly, as occurs for instance in the suppression of superconductivity in $La_{2-x}Ba_xCuO_4$ at $x=0.125$[8] and the metal-insulator transition in $La_{1-x}L_xNiO_3$.[9] In the latter case the *M-I* transition has been attributed to the band narrowing which occurs when the metal-oxygen-metal angle between neighboring octahedra bends away from the ideal 180°, decreasing metal-*d*–oxygen-*p* overlap. The present results for $Sr_2Ir_{1-x}Ru_xO_4$ look remarkably like that: the structural change at $x\sim 0.6$ could represent the straightening of the *M*-O-*M* bonds from the buckled case of Sr_2IrO_4 to the ideal case of Sr_2RuO_4. The implication is that the hybridization of Ir and Ru with oxygen is as essential to the properties of these materials as it is to cuprates and nickelates.

CONCLUSIONS

The magnetic character of Ru ions in oxides has long been the subject of research and discussion.[3,4,10–13] $S=1$ Ru^{4+} is apparently exclusively observed, consistent with our measured Ru moment for low x in $Sr_2Ir_{1-x}Ru_xO_4$. The magnetism of the $CaRuO_3$-$SrRuO_3$ perovskite solid solution[3,4] is more typical of the general behavior: the ferromagnetic T_c of $SrRuO_3$ decreases with increasing Ca content in $Sr_{1-x}Ca_xRuO_3$, until at approximately $x=0.5$, the ordered magnetic state disappears and the materials are paramagnetic. The $Sr_{1-x}Ca_xRuO_3$ solid solution displays metallic conductivity for all x, and *the full Curie moment for Ru above T_c is maintained for all compositions,* in distinct contrast to our observed metal-insulator itinerant-localized transition for $Sr_2Ir_{1-x}Ru_xO_4$. The magnetic states in $SrRuO_3$ and Sr_2RuO_4 appear to be considerably different. It is tempting to associate the difference with the difference between the three-dimensional structure of $SrRuO_3$ and the two-dimensional structure of Sr_2RuO_4. It is surprising, however, that we find the electrons to be more itinerant in two-dimensional Sr_2RuO_4 than in three-dimensional $SrRuO_3$, which does not conform with the general expectation. Further experiments comparing the present materials to the cuprates, or to early-transition-metal perovskites undergoing metal-insulator transitions[14] would be of interest. If, in addition, as the present results suggest, the bending of the Ir-O-Ir bond, reducing Ir-5*d*–oxygen-2*p* overlap, is critical to the electronic properties, then an explanation may be provided for the enigmatic insulating character of Sr_2IrO_4.

[1]J. B. Goodenough and J. M. Longo, in *Magnetic and Other Properties of Oxides and Related Compounds,* edited by K.-H. Hellwege, Landolt-Börnstein New Series, Group III, Vol. 4a (Springer-Verlag, Berlin, 1970), p. 126.
[2]W. D. Komer and D. J. Machin, J. Less-Common Met. **61**, 91 (1978).
[3]T. C. Gibb, R. Greatrex, N. N. Greenwood, D. C. Puxley, and K. G. Snowdon, J. Solid State Chem. **11**, 17 (1974).
[4]A. Kanbayasi, J. Phys. Soc. Jpn. **44**, 108 (1978).
[5]J. J. Randall, Jr., L. Katz, and R. Ward, J. Am. Chem. Soc. **79**, 266 (1957).
[6]J. J. Randall and R. Ward, J. Am. Chem. Soc. **81**, 2629 (1959).
[7]F. Lichtenberg, A. Catana, J. Mannhart, and D. G. Schlom, Appl. Phys. Lett. **60**, 1138 (1992).
[8]J. D. Axe, A. H. Moudden, D. Hohlwein, D. E. Cox, K. M. Mohanty, A. R. Moodenbaugh, and Y. Xu, Phys. Rev. Lett. **62**, 2751 (1989).
[9]J. B. Torrance, P. Lacorre, A. I. Nazzal, E. J. Ansaldo, and Ch. Niedermayer, Phys. Rev. B **45**, 8209 (1992).
[10]J. B. Goodenough, Mat. Res. Bull. **6**, 967 (1971).
[11]J. M. Longo, P. M. Raccah, and J. B. Goodenough, J. Appl. Phys. **39**, 1327 (1968).
[12]P. D. Battle, J. B. Goodenough, and R. Price, J. Solid State Chem. **46**, 234 (1983).
[13]P. A. Cox, R. G. Egdell, J. B. Goodenough, A. Hammett, and C. C. Naish, J. Phys. C **16**, 6221 (1983).
[14]K. Kumagai, T. Suzuki, Y. Taguchi, Y. Okada, Y. Fujishima, and Y. Tokura, Phys. Rev. B **48**, 7636 (1993).